Electronic Supplementary Material (ESI) for Physical Chemistry Chemical Physics.

Electric Dipole Moments and Chemical Bonding of Diatomic Alkali - Alkaline Earth Molecules – Electronic Supplementary Information

Johann V. Pototschnig,* Andreas W. Hauser, and Wolfgang E. Ernst*

Graz University of Technology, Institute of Experimental Physics, Petersgasse 16, 8010 Graz, Austria.

E-mail: johann.pototschnig@tugraz.at; wolfgang.ernst@tugraz.at

Section 1 of this ESI contains several additional tables providing more detailed information on the ab initio results. Some of these results are displayed as figures in the manuscript. In Section 1.1 predicted values of the formula in the text are compared to previous calculations. Additional orbital pictures are plotted in Section 2, which support the explanation in the manuscript.

Section 1.2 contains the results of a multiconfigurational self consistent field calculation (MC-SCF) in combination with an multireference configuration interaction (MRCI) for 16 different alkali-alkaline earth molecules. Details of the calculation can be found in the manuscript. The number of orbitals and states considered in the calculation are given in Section 1.6. Tabulated values describing the convergence of the dissociation energies for large internuclear separations and corresponding distances are listed in Section 1.3. Results without using the core polarization potentials (CPP) are given in Section 1.4 and for large internuclear distances in Section 1.5. The finite field values are listed in Section 1.7 together with applied field strengths. Section 1.8 gives

*To whom correspondence should be addressed

a comparison between the results for the equilibrium internuclear separations found in Section 1.2 and the tabulated covalent and van der Walls radii. The calculated polarizabilities (Section 1.7) are compared to the mean of the atomic polarizabilities in Section 1.9. The next two sections are concerned with comparisons between calculations with and without a CPP (Section 1.10) and between results obtained by the MRCI program and by finite field calculations (Section 1.11). In Section 1.13 the literature values for atomic properties are listed.

Contents

1 Tables

1.1 Predictions obtained with the Empirical Model and Previous Results for Additional Molecules

Table 1: In this table the predicted values for the $^2\Sigma^+$ state of several AK-AKE molecules are listed alongside previous results obtained by *ab initio* calculations. The results are depicted in Fig. 8 in the manuscript.

mol.	Ref.	μ_e/D	r_e/Å	D_e/cm^{-1}	ω_e/cm^{-1}
LiBa	pred.	0.07		3646	
	1	-0.37	3.67	2871	205.5
	2	-0.52	3.73	3646	204.1
	3		3.58	3146	200.7
NaBa	pred.	0.16		2573	
	2	0.25	4.12	2573	92.3
	4		3.87	1920	89.2
KBa	pred.	2.27		1750	
	2	1.62	4.65	1750	59.4
RbBa	pred.	2.09		1472	
	2	3.32	4.93	1472	39.2
CsBe	pred.	2.22		776	
CsMg	pred.	1.45		729	
	5	0.83	4.54	544	43.2
CsCa	pred.	2.55		1282	
CsSr	pred.	2.22		1205	
	6	1.91	4.79	1084	33.8
CsBa	pred.	2.72		1466	
	2	4.02	5.19	1466	32.8
FrBe	pred.	1.94		764	
FrMg	pred.	1.25		726	
FrCa	pred.	2.46		1262	
FrSr	pred.	2.18		1183	
FrBa	pred.	2.54		1301	

1.2 Multireference Configuration Interaction

1.2.1 $^2\Sigma^+$ state

Table 2: Permanent electric dipole moment of the $^2\Sigma^+$ state for the sixteen AK-AKE molecules in the test set as determined by MCSCF+MRCI calculations.

μ_e / D	Be	Mg	Ca	Sr
Li	3.460	1.141	1.123	0.175
Na	2.292	0.867	1.167	0.462
K	2.230	1.082	2.170	1.555
Rb	2.023	1.053	2.276	1.705

Table 3: Dissociation energy of the $^2\Sigma^+$ state for the sixteen AK-AKE molecules in the test set as determined by MCSCF+MRCI calculations.

D_e / cm^{-1}	Be	Mg	Ca	Sr
Li	2427	1538	2613	2471
Na	1291	946	1792	1728
K	920	779	1455	1358
Rb	816	744	1337	1279

Table 4: Equilibrium internuclear separation of the $^2\Sigma^+$ state for the sixteen AK-AKE molecules in the test set as determined by MCSCF+MRCI calculations.

r_e / Å	Be	Mg	Ca	Sr
Li	2.601	3.102	3.388	3.572
Na	2.966	3.465	3.665	3.843
K	3.506	3.994	4.196	4.392
Rb	3.704	4.173	4.369	4.564

Table 5: Vibrational constant of the $^2\Sigma^+$ state for the sixteen AK-AKE molecules in the test set as determined by MCSCF+MRCI calculations.

ω_e / cm^{-1}	Be	Mg	Ca	Sr
Li	312.9	181.0	199.8	180.7
Na	173.0	89.6	102.9	87.2
K	121.7	64.3	71.3	56.7
Rb	104.2	54.1	57.0	42.6

Table 6: Anharmonicity parameter of the $^2\Sigma^+$ state for the sixteen AK-AKE molecules in the test set as determined by MCSCF+MRCI calculations.

$\omega_e x_e$ / cm^{-1}	Be	Mg	Ca	Sr
Li	10.15	5.33	3.82	3.31
Na	5.80	2.13	1.48	1.10
K	4.03	1.32	0.87	0.59
Rb	3.32	0.98	0.61	0.35

Table 7: Fraction of ionic character of the $^2\Sigma^+$ state for the sixteen AK-AKE molecules in the test set as determined by MCSCF+MRCI calculations.

f_{Ion} / %	Be	Mg	Ca	Sr
Li	52	14	13	2
Na	30	10	13	5
K	25	11	20	14
Rb	21	10	20	15

1.2.2 $^4\Sigma^+$ state

Table 8: Permanent electric dipole moment of the $^4\Sigma^+$ state for the sixteen AK-AKE molecules in the test set as determined by MCSCF+MRCI calculations.

μ_e / D	Be	Mg	Ca	Sr
Li	-0.621	-2.537	-4.640	-6.703
Na	-0.453	-0.988	-1.593	-2.040
K	-0.733	-1.652	-2.612	-3.008
Rb	-0.789	-1.628	-2.204	-2.710

Table 9: Dissociation energy of the $^4\Sigma^+$ state for the sixteen AK-AKE molecules in the test set as determined by MCSCF+MRCI calculations.

D_e / cm^{-1}	Be	Mg	Ca	Sr
Li	59	222	522	692
Na	50	131	237	287
K	48	157	343	376
Rb	47	170	316	343

Table 10: Equilibrium internuclear separation of the $^4\Sigma^+$ state for the sixteen AK-AKE molecules in the test set as determined by MCSCF+MRCI calculations.

r_e / Å	Be	Mg	Ca	Sr
Li	5.505	4.715	4.593	4.589
Na	5.837	5.713	5.736	5.807
K	5.992	5.731	5.727	5.947
Rb	6.027	5.844	6.054	6.148

Table 11: Vibrational constant of the $^4\Sigma^+$ state for the sixteen AK-AKE molecules in the test set as determined by MCSCF+MRCI calculations.

ω_e / cm^{-1}	Be	Mg	Ca	Sr
Li	24.7	31.9	54.5	61.4
Na	18.3	20.6	23.6	22.9
K	16.2	19.9	25.6	21.6
Rb	15.3	17.7	19.2	16.3

Table 12: Anharmonicity parameter of the $^4\Sigma^+$ state for the sixteen AK-AKE molecules in the test set as determined by MCSCF+MRCI calculations.

$\omega_e x_e$ / cm^{-1}	Be	Mg	Ca	Sr
Li	2.79	1.14	1.42	1.36
Na	1.68	0.81	0.59	0.46
K	1.37	0.63	0.48	0.31
Rb	1.25	0.47	0.29	0.19

Table 13: Fraction of ionic character of the $^4\Sigma^+$ state for the sixteen AK-AKE molecules in the test set as determined by MCSCF+MRCI calculations.

f_{Ion} / %	Be	Mg	Ca	Sr
Li	4	21	40	57
Na	3	7	11	14
K	5	11	18	20
Rb	5	11	14	17

1.3 Multireference Configuration Interaction - asymptotic convergence

Table 14: Largest internuclear distances calculated to check asymptotic convergence in the MSC-SCF+MRCI calculations.

r_{max} / Å	Be	Mg	Ca	Sr
Li	11	13	10	10
Na	10	12	11	11
K	10.5	12	30	25
Rb	10.5	10	11	13

1.3.1 $^2\Sigma^+$ state

Table 15: Dissociation energy of the $^2\Sigma^+$ state for the sixteen AK-AKE molecules in the test set as determined by MCSCF+MRCI calculations with the asymptotic distances given in Table 14.

D_e / cm^{-1}	Be	Mg	Ca	Sr
Li	2429	1542	2613	2470
Na	1291	949	1797	1735
K	921	787	1476	1383
Rb	817	744	1348	1301

Table 16: Differences in the dissociation energy of the $^2\Sigma^+$ state for the MCSCF+MRCI calculations between asymptotic limits of 10 Å and the distances given in Table 14.

ΔD_e / cm^{-1}	Be	Mg	Ca	Sr
Li	2	4	0	-1
Na	0	3	5	7
K	1	8	21	25
Rb	1	0	11	22

1.3.2 $^4\Sigma^+$ state

Table 17: Dissociation energy of the $^4\Sigma^+$ state for the sixteen AK-AKE molecules in the test set as determined by MCSCF+MRCI calculations with the asymptotic distances given in Table 14.

D_e / cm^{-1}	Be	Mg	Ca	Sr
Li	61	229	522	692
Na	50	138	246	302
K	49	173	381	427
Rb	47	170	334	387

Table 18: Differences in the dissociation energy of the $^4\Sigma^+$ state for the MCSCF+MRCI calculations between asymptotic limits of 10 Å and the distances given in Table 14.

ΔD_e / cm^{-1}	Be	Mg	Ca	Sr
Li	2	7	0	0
Na	0	7	9	15
K	1	16	38	51
Rb	0	0	18	44

1.4 Multireference Configuration Interaction without CPPs

1.4.1 $^2\Sigma^+$ state

Table 19: Permanent electric dipole moment of the $^2\Sigma^+$ state for the sixteen AK-AKE molecules in the test set as determined by MCSCF+MRCI calculations without CPPs.

μ_e / D	Be	Mg	Ca	Sr
Li	3.460	1.297	1.312	0.395
Na	2.403	1.090	1.602	0.919
K	2.564	1.596	3.337	2.831
Rb	2.470	1.744	3.807	3.360

Table 20: Dissociation energy of the $^2\Sigma^+$ state for the sixteen AK-AKE molecules in the test set as determined by MCSCF+MRCI calculations without CPPs.

D_e / cm^{-1}	Be	Mg	Ca	Sr
Li	2427	1648	2883	2870
Na	1223	953	1862	1882
K	823	744	1426	1425
Rb	695	659	1299	1288

Table 21: Equilibrium internuclear separation of the $^2\Sigma^+$ state for the sixteen AK-AKE molecules in the test set as determined by MCSCF+MRCI calculations without CPPs.

r_e / Å	Be	Mg	Ca	Sr
Li	2.601	3.098	3.385	3.573
Na	3.034	3.547	3.750	3.930
K	3.644	4.162	4.361	4.561
Rb	3.881	4.396	4.578	4.782

Table 22: Vibrational constant of the $^2\Sigma^+$ state for the sixteen AK-AKE molecules in the test set as determined by MCSCF+MRCI calculations without CPPs.

ω_e / cm^{-1}	Be	Mg	Ca	Sr
Li	312.9	187.7	208.7	190.3
Na	163.8	87.3	102.4	89.0
K	108.9	59.5	68.6	56.1
Rb	90.0	48.1	54.3	42.3

Table 23: Anharmonicity parameter of the $^2\Sigma^+$ state for the sixteen AK-AKE molecules in the test set as determined by MCSCF+MRCI calculations without CPPs.

$\omega_e x_e$ / cm^{-1}	Be	Mg	Ca	Sr
Li	10.10	5.35	3.78	3.16
Na	5.48	2.00	1.41	1.05
K	3.60	1.19	0.82	0.55
Rb	2.91	0.88	0.57	0.33

Table 24: Fraction of ionic character of the $^2\Sigma^+$ state for the sixteen AK-AKE molecules in the test set as determined by MCSCF+MRCI calculations without CPPs.

f_{Ion} / %	Be	Mg	Ca	Sr
Li	52	16	15	4
Na	31	12	17	9
K	28	15	30	24
Rb	25	16	33	28

1.4.2 $^4\Sigma^+$ state

Table 25: Permanent electric dipole moment of the $^4\Sigma^+$ state for the sixteen AK-AKE molecules in the test set as determined by MCSCF+MRCI calculations without CPPs.

μ_e / D	Be	Mg	Ca	Sr
Li	-0.621	-2.507	-4.501	-5.286
Na	-0.508	-1.170	-1.956	-2.317
K	-0.922	-2.159	-2.949	-3.511
Rb	-0.938	-2.094	-2.768	-3.258

Table 26: Dissociation energy of the $^4\Sigma^+$ state for the sixteen AK-AKE molecules in the test set as determined by MCSCF+MRCI calculations without CPPs.

D_e / cm^{-1}	Be	Mg	Ca	Sr
Li	59	215	521	620
Na	48	138	271	320
K	50	181	315	429
Rb	45	183	287	388

Table 27: Equilibrium internuclear separation of the $^4\Sigma^+$ state for the sixteen AK-AKE molecules in the test set as determined by MCSCF+MRCI calculations without CPPs.

r_e / Å	Be	Mg	Ca	Sr
Li	5.506	4.750	4.613	4.773
Na	5.872	5.705	5.675	5.788
K	6.023	5.699	5.906	5.992
Rb	6.189	5.884	6.145	6.244

Table 28: Vibrational constant of the $^4\Sigma^+$ state for the sixteen AK-AKE molecules in the test set as determined by MCSCF+MRCI calculations without CPPs.

ω_e / cm^{-1}	Be	Mg	Ca	Sr
Li	25.7	30.1	60.9	58.9
Na	17.7	20.9	25.9	24.4
K	15.6	21.1	24.1	23.3
Rb	13.8	18.9	19.3	17.7

Table 29: Anharmonicity parameter of the $^4\Sigma^+$ state for the sixteen AK-AKE molecules in the test set as determined by MCSCF+MRCI calculations without CPPs.

$\omega_e x_e$ / cm^{-1}	Be	Mg	Ca	Sr
Li	2.79	1.05	1.78	1.40
Na	1.62	0.79	0.62	0.47
K	1.20	0.62	0.46	0.32
Rb	1.06	0.49	0.32	0.20

Table 30: Fraction of ionic character of the $^4\Sigma^+$ state for the sixteen AK-AKE molecules in the test set as determined by MCSCF+MRCI calculations without CPPs.

f_{Ion} / %	Be	Mg	Ca	Sr
Li	4	21	38	44
Na	3	8	14	16
K	6	15	20	23
Rb	6	14	18	21

1.5 Multireference Configuration Interaction without CPPs - asymptotic convergence

Table 31: Largest internuclear distances calculated to check asymptotic convergence in the MSC-SCF+MRCI calculations without CPPs.

r_{max} / Å	Be	Mg	Ca	Sr
Li	11	100	100	100
Na	100	12	100	10
K	13	13	100	100
Rb	100	100	10.5	10

1.5.1 $^2\Sigma^+$ state

Table 32: Dissociation energy of the $^2\Sigma^+$ state for the sixteen AK-AKE molecules in the test set as determined by MCSCF+MRCI calculations without CPPs with the asymptotic distances given in Table 31.

D_e / cm^{-1}	Be	Mg	Ca	Sr
Li	2429	1653	2896	2885
Na	1227	957	1872	1882
K	829	754	1457	1459
Rb	700	671	1307	1288

Table 33: Differences in the dissociation energy of the $^2\Sigma^+$ state for the MCSCF+MRCI calculations without CPPs between asymptotic distances of 10 Å and the values given in Table 31.

ΔD_e / cm^{-1}	Be	Mg	Ca	Sr
Li	2	5	13	15
Na	4	4	10	0
K	6	10	31	34
Rb	5	12	8	0

1.5.2 $^4\Sigma^+$ state

Table 34: Dissociation energy of the $^4\Sigma^+$ state for the sixteen AK-AKE molecules in the test set as determined by MCSCF+MRCI calculations without CPPs with the asymptotic distances given in Table 31.

D_e / cm^{-1}	Be	Mg	Ca	Sr
Li	61	223	541	644
Na	51	141	294	320
K	52	151	358	488
Rb	35	193	300	388

Table 35: Differences in the dissociation energy of the $^4\Sigma^+$ state for the MCSCF+MRCI calculations without CPPs between asymptotic distances of 10 Å and the values given inTable 31.

ΔD_e / cm^{-1}	Be	Mg	Ca	Sr
Li	2	8	20	24
Na	3	3	23	0
K	2	-30	43	59
Rb	-10	10	13	0

1.6 Technical details of the Multiconfigurational Calculations

In this section we give details about orbital occupation and calculated states. The calculations were performed in the C_{2v} point group and the labels A_1, B_1, B_2, and A_2 refer to the irreducible representations.

Table 36: The number of closed orbitals are listed for the different molecules in the MCSCF and MRCI calculations.

	Be				Mg				Ca				Sr			
	A_1	B_1	B_2	A_2	A_1	B_1	B_2	A_2	A_1	B_1	B_2	A_2	A_1	B_1	B_2	A_2
Li	2				4	1	1		3	1	1		3	1	1	
Na	4	1	1		6	2	2		5	2	2		5	2	2	
K	3	1	1		5	2	2		4	2	2		4	2	2	
Rb	3	1	1		5	2	2		4	2	2		4	2	2	

Table 37: The number of occupied orbitals are listed for the different molecules in the MCSCF and MRCI calculations.

	Be				Mg				Ca				Sr			
	A_1	B_1	B_2	A_2	A_1	B_1	B_2	A_2	A_1	B_1	B_2	A_2	A_1	B_1	B_2	A_2
Li	11	4	4	1	13	5	5	1	12	5	5	1	12	5	5	1
Na	12	5	5	1	17	7	7	2	16	8	8	2	13	5	5	1
K	14	6	6	2	16	7	7	2	13	6	6	2	13	6	6	2
Rb	15	7	7	3	15	7	7	2	16	8	8	3	13	6	6	2

1.6.1 $^2\Sigma^+$ state

Table 38: The number of states determined in the MCSCF for the doublet multiplicity are given.

	Be				Mg				Ca				Sr			
	A_1	B_1	B_2	A_2	A_1	B_1	B_2	A_2	A_1	B_1	B_2	A_2	A_1	B_1	B_2	A_2
Li	9	5	5	1	9	5	5	1	11	6	6	3	12	6	6	2
Na	7	4	4	1	10	5	5	2	12	7	7	3	10	5	5	2
K	10	5	5	2	10	5	5	2	8	4	4	2	8	4	4	2
Rb	11	6	6	3	13	8	8	3	11	6	6	3	10	5	5	2

Table 39: The number of states determined in the MRCI for the doublet multiplicity are given.

	Be				Mg				Ca				Sr			
	A_1	B_1	B_2	A_2	A_1	B_1	B_2	A_2	A_1	B_1	B_2	A_2	A_1	B_1	B_2	A_2
Li	5	3	3	1	5	3	3	1	7	4	4	1	5	3	3	1
Na	6	3	3	1	6	3	3	1	7	4	4	2	7	4	4	2
K	7	4	4	1	7	4	4	1	6	3	3	1	5	3	3	1
Rb	7	4	4	1	6	3	3	1	6	5	5	1	7	4	4	2

1.6.2 $^4\Sigma^+$ state

Table 40: The number of states determined in the MCSCF for the quartet multiplicity are given.

	Be				Mg				Ca				Sr			
	A_1	B_1	B_2	A_2	A_1	B_1	B_2	A_2	A_1	B_1	B_2	A_2	A_1	B_1	B_2	A_2
Li	1	1	1		1	1	1		3	2	2	1	3	2	2	1
Na	1	1	1		1	1	1		3	2	2	1	3	2	2	1
K	1	1	1		1	1	1		3	2	2	1	3	2	2	1
Rb	1	1	1		1	1	1		3	2	2	1	3	2	2	1

Table 41: The number of states determined in the MRCI for the quartet multiplicity are given.

	Be				Mg				Ca				Sr			
	A_1	B_1	B_2	A_2	A_1	B_1	B_2	A_2	A_1	B_1	B_2	A_2	A_1	B_1	B_2	A_2
Li	1	1	1		1	1	1		3	2	2	1	3	2	2	1
Na	1	1	1		1	1	1		3	2	2	1	3	2	2	1
K	1	1	1		1	1	1		3	2	2	1	3	2	2	1
Rb	1	1	1		1	1	1		1	1	1		3	2	2	1

1.7 Finite Field Calculations

1.7.1 $^2\Sigma^+$ state

Table 42: Permanent electric dipole moment of the $^2\Sigma^+$ state for the sixteen AK-AKE molecules in the test set as determined by finite field calculations for MCSCF+MRCI results.

μ_e / D	Be	Mg	Ca	Sr
Li	3.467	1.184	1.192	0.285
Na	2.326	0.857	1.182	0.511
K	2.219	1.083	2.122	1.523
Rb	1.970	1.037	2.188	1.645

Table 43: Polarizabilities along the internuclear axis of the $^2\Sigma^+$ state for the sixteen AK-AKE molecules in the test set as determined by finite field calculations for MCSCF+MRCI results.

$\alpha_{\|\|}$ / a. u.	Be	Mg	Ca	Sr
Li	365	470	588	653
Na	397	432	577	636
K	628	656	869	925
Rb	631	664	922	972

Table 44: Field strength for the finite field calculation of the $^2\Sigma^+$ state properties.

field / a. u.	Be	Mg	Ca	Sr
Li	2.50E-04	2.50E-04	5.00E-05	2.50E-04
Na	1.25E-04	2.50E-04	2.50E-04	1.25E-04
K	1.25E-04	5.00E-05	2.50E-04	2.50E-05
Rb	1.25E-04	1.25E-04	5.00E-05	1.25E-04

1.7.2 $^4\Sigma^+$ state

Table 45: Permanent electric dipole moment of the $^4\Sigma^+$ state for the sixteen AK-AKE molecules in the test set as determined by finite field calculations for MCSCF+MRCI results.

μ_e / D	Be	Mg	Ca	Sr
Li	-0.613	-2.519	-4.578	-6.606
Na	-0.452	-0.986	-1.619	-2.003
K	-0.719	-1.581	-2.501	-2.989
Rb	-0.790	-1.662	-2.130	-2.661

Table 46: Polarizabilities along the internuclear axis of the $^4\Sigma^+$ state for the sixteen AK-AKE molecules in the test set as determined by finite field calculations for MCSCF+MRCI results.

$\alpha_{\|\|}$ / a. u.	Be	Mg	Ca	Sr
Li	223	423	1031	1340
Na	229	326	686	1200
K	300	338	950	1523
Rb	363	645	922	1491

Table 47: Field strength for the finite field calculation of the $^4\Sigma^+$ state properties.

field / a. u.	Be	Mg	Ca	Sr
Li	1.25E-04	2.50E-04	1.25E-04	1.25E-04
Na	1.25E-04	1.25E-04	2.50E-05	1.25E-04
K	5.00E-05	5.00E-05	5.00E-05	1.25E-04
Rb	5.00E-05	2.50E-05	3.75E-05	1.25E-05

1.8 Radii

Table 48: Covalent radii for the sixteen AK-AKE molecules in the test set as determined with tabulated values.[7]

r_{cov} / Å	Be	Mg	Ca	Sr
Li	2.24	2.69	3.04	3.23
Na	2.62	3.07	3.42	3.61
K	2.99	3.44	3.79	3.98
Rb	3.16	3.61	3.96	4.15

Table 49: Van der Waals radii for the sixteen AK-AKE molecules in the test set as determined with tabulated values.[8]

r_{vdW} / Å	Be	Mg	Ca	Sr
Li	4.10	4.63	4.74	4.96
Na	4.48	5.01	5.12	5.34
K	4.71	5.24	5.35	5.57
Rb	5.19	5.72	5.83	6.05

1.8.1 $^2\Sigma^+$ state

Table 50: Difference between the covalent radii (Table 48) and the equilibrium internuclear separation of the $^2\Sigma^+$ state (Table 4) for the sixteen AK-AKE molecules in the test set.

r_e-r_{cov} / Å	Be	Mg	Ca	Sr
Li	0.36	0.41	0.35	0.34
Na	0.35	0.40	0.25	0.23
K	0.52	0.55	0.41	0.41
Rb	0.54	0.56	0.41	0.41

Table 51: Difference between the van der Waals radii (Table 49) and the equilibrium internuclear separation of the $^2\Sigma^+$ state (Table 4) for the sixteen AK-AKE molecules in the test set.

r_{vdW}-r_e / Å	Be	Mg	Ca	Sr
Li	1.50	1.53	1.35	1.39
Na	1.51	1.55	1.46	1.50
K	1.20	1.25	1.15	1.18
Rb	1.49	1.55	1.46	1.49

1.8.2 $^4\Sigma^+$ state

Table 52: Difference between the covalent radii (Table 48) and the equilibrium internuclear separation of the $^4\Sigma^+$ state (Table 10) for the sixteen AK-AKE molecules in the test set.

r_e-r_{cov} / Å	Be	Mg	Ca	Sr
Li	3.27	2.03	1.55	1.36
Na	3.22	2.64	2.32	2.20
K	3.00	2.29	1.94	1.97
Rb	2.87	2.23	2.09	2.00

Table 53: Difference between the van der Waals radii (Table 49) and the equilibrium internuclear separation of the $^4\Sigma^+$ state (Table 10) for the sixteen AK-AKE molecules in the test set.

r_{vdW}-r_e / Å	Be	Mg	Ca	Sr
Li	-1.41	-0.09	0.15	0.37
Na	-1.36	-0.70	-0.62	-0.47
K	-1.28	-0.49	-0.38	-0.38
Rb	-0.84	-0.12	-0.22	-0.10

1.9 Polarizabilities

Table 54: Mean of the atomic polarizabilities using tabulated values.[9]

α_{atom} / a. u.	Be	Mg	Ca	Sr
Li	101	118	167	175
Na	100	117	166	174
K	164	181	230	238
Rb	178	195	244	252

1.9.1 $^2\Sigma^+$ state

Table 55: Factor between the atomic polarizabilities (Table 54) and the polarizabilities along the internuclear axis of the $^2\Sigma^+$ state for the sixteen AK-AKE molecules in the test set as determined by finite field calculations for MCSCF+MRCI results (Table 43).

$\alpha_{\parallel}/\alpha_{atom}$ / a. u.	Be	Mg	Ca	Sr
Li	3.62	3.98	3.53	3.73
Na	3.96	3.69	3.48	3.65
K	3.82	3.62	3.78	3.88
Rb	3.54	3.40	3.78	3.85

1.9.2 $^4\Sigma^+$ state

Table 56: Factor between the atomic polarizabilities (Table 54) and the polarizabilities along the internuclear axis of the $^4\Sigma^+$ state for the sixteen AK-AKE molecules in the test set as determined by finite field calculations for MCSCF+MRCI results (Table 46).

$\alpha_{\parallel}/\alpha_{atom}$ / a. u.	Be	Mg	Ca	Sr
Li	2.21	3.59	6.19	7.65
Na	2.29	2.78	4.14	6.88
K	1.83	1.86	4.13	6.39
Rb	2.04	3.30	3.78	5.91

1.10 Geometry and Energy Comparisons: With and Without CPPs

1.10.1 $^2\Sigma^+$ state

Table 57: Differences in the permanent electric dipole moments of the $^2\Sigma^+$ state for the sixteen AK-AKE molecules in the test set as determined by MCSCF+MRCI calculations with (Table 2) and without (Table 19) CPPs.

μ_e(no CPP)-μ_e(with CPP) / D	Be	Mg	Ca	Sr
Li	0.000	0.156	0.189	0.220
Na	0.111	0.223	0.435	0.456
K	0.334	0.515	1.167	1.276
Rb	0.447	0.691	1.531	1.655

Table 58: Difference in the dissociation energies of the $^2\Sigma^+$ state for the sixteen AK-AKE molecules in the test set as determined by MCSCF+MRCI calculations with (Table 3) and without (Table 20) CPPs.

D_e(no CPP)-D_e(with CPP) / cm^{-1}	Be	Mg	Ca	Sr
Li	0	110	270	399
Na	-68	7	70	154
K	-97	-35	-29	67
Rb	-121	-85	-38	9

Table 59: Difference in equilibrium internuclear separation of the $^2\Sigma^+$ state for the sixteen AK-AKE molecules in the test set as determined by MCSCF+MRCI calculations with (Table 4) and without (Table 21) CPPs.

r_e(no CPP)-r_e(with CPP) / Å	Be	Mg	Ca	Sr
Li	0.000	-0.004	-0.003	0.001
Na	0.068	0.082	0.085	0.087
K	0.138	0.168	0.165	0.169
Rb	0.177	0.223	0.209	0.218

1.10.2 $^4\Sigma^+$ state

Table 60: Differences in the permanent electric dipole moments of the $^4\Sigma^+$ state for the sixteen AK-AKE molecules in the test set as determined by MCSCF+MRCI calculations with (Table 8) and without (Table 25) CPPs.

μ_e(no CPP)-μ_e(with CPP) / D	Be	Mg	Ca	Sr
Li	0.000	0.030	0.152	1.418
Na	-0.056	-0.182	-0.364	-0.276
K	-0.189	-0.507	-0.338	-0.503
Rb	-0.150	-0.466	-0.564	-0.547

Table 61: Difference in the dissociation energies of the $^4\Sigma^+$ state for the sixteen AK-AKE molecules in the test set as determined by MCSCF+MRCI calculations with (Table 9) and without (Table 26) CPPs.

D_e(no CPP)-D_e(with CPP) / cm^{-1}	Be	Mg	Ca	Sr
Li	0	-7	-1	-72
Na	-2	7	34	33
K	2	24	-28	53
Rb	-2	13	-29	45

Table 62: Difference in equilibrium internuclear separation of the $^4\Sigma^+$ state for the sixteen AK-AKE molecules in the test set as determined by MCSCF+MRCI calculations with (Table 10) and without (Table 27) CPPs.

r_e(no CPP)-r_e(with CPP) / Å	Be	Mg	Ca	Sr
Li	0.001	0.035	0.020	0.184
Na	0.035	-0.008	-0.061	-0.019
K	0.031	-0.032	0.179	0.045
Rb	0.162	0.040	0.091	0.096

1.11 Comparison between Internally Evaluated MRCI Permanent Electric Dipole Moments and Finite Field Results

1.11.1 $^2\Sigma^+$ state

Table 63: Differences in the permanent electric dipole moments of the $^2\Sigma^+$ state for the sixteen AK-AKE molecules in the test set as determined by the MRCI routine (Table 2) and by finite field calculations (Table 42).

μ_e(FF)-μ_e(MRCI) / D	Be	Mg	Ca	Sr
Li	0.007	0.044	0.069	0.110
Na	0.034	-0.011	0.015	0.048
K	-0.011	0.001	-0.047	-0.033
Rb	-0.053	-0.016	-0.087	-0.061

1.11.2 $^4\Sigma^+$ state

Table 64: Differences in the permanent electric dipole moments of the $^4\Sigma^+$ state for the sixteen AK-AKE molecules in the test set as determined by the MRCI routine (Table 8) and by finite field calculations (Table 45).

μ_e(FF)-μ_e(MRCI) / D	Be	Mg	Ca	Sr
Li	0.008	0.018	0.075	0.097
Na	0.000	0.002	-0.026	0.037
K	0.013	0.071	0.111	0.019
Rb	-0.002	-0.035	0.074	0.049

1.12 Vibrational Averaged Permanent Electric Dipole Moment

1.12.1 $^2\Sigma^+$ state

Table 65: Vibrational averaged permanent electric dipole moment of the $^2\Sigma^+$ state for the sixteen AK-AKE molecules in the test set as determined by MCSCF+MRCI calculations.

μ_0 / D	Be	Mg	Ca	Sr
Li	3.377	1.103	1.104	0.169
Na	2.216	0.844	1.153	0.458
K	2.150	1.061	2.146	1.544
Rb	1.953	1.037	2.255	1.695

Table 66: Change of the permanent electric dipole moment by vibrational averaging. (see Table 2 and Table 65)

$\mu_e - \mu_0$ / D	Be	Mg	Ca	Sr
Li	0.083	0.038	0.019	0.007
Na	0.075	0.022	0.014	0.004
K	0.079	0.020	0.023	0.012
Rb	0.069	0.017	0.021	0.011

1.12.2 $^4\Sigma^+$ state

Table 67: Vibrational averaged permanent electric dipole moment of the $^4\Sigma^+$ state for the sixteen AK-AKE molecules in the test set as determined by MCSCF+MRCI calculations.

μ_0 / D	Be	Mg	Ca	Sr
Li	-0.575	-2.421	-4.514	-6.498
Na	-0.422	-0.957	-1.558	-2.007
K	-0.688	-1.606	-2.500	-2.922
Rb	-0.739	-1.585	-2.169	-2.713

Table 68: Change of the permanent electric dipole moment by vibrational averaging. (see Table 8 and Table 67)

$\mu_e - \mu_0$ / D	Be	Mg	Ca	Sr
Li	-0.046	-0.116	-0.126	-0.205
Na	-0.031	-0.031	-0.034	-0.033
K	-0.045	-0.046	-0.111	-0.087
Rb	-0.050	-0.043	-0.035	0.003

1.13 Atomic Properties as obtained from Literature

Table 69: The literature values[10] for differences in the lowest excitation energies are listed. These values are depicted in Fig. 1 in the manuscript. For Ba and Ra the lowest ^3P state was used.

ΔE_{ex} / cm^{-1}	Be	Mg	Ca	Sr	Ba	Ra
Li	7076	6987	359	-201	-1821	487
Na	5013	4923	-1705	-2265	-3884	-1577
K	8957	8867	2239	1679	60	2367
Rb	9243	9154	2526	1965	346	2654
Cs	10433	10343	3715	3155	1536	3843
Fr	8618	8529	1901	1341	-279	2029

Table 70: The literature values[11] for differences in electronegativities are listed. These values are depicted in Fig. 1 in the manuscript.

ΔEN / Pauling	Be	Mg	Ca	Sr	Ba	Ra
Li	0.59	0.33	0.02	-0.03	-0.09	-0.08
Na	0.64	0.38	0.07	0.02	-0.04	-0.03
K	0.75	0.49	0.18	0.13	0.07	0.08
Rb	0.75	0.49	0.18	0.13	0.07	0.08
Cs	0.78	0.52	0.21	0.16	0.1	0.11
Fr	0.87	0.61	0.3	0.25	0.19	0.2

2 Isosurface Plots of Molecular Orbitals

Isosurfaces of the first three partly occupied orbitals in the irreducible representation A_1 in the C_{2v} point group are displayed. The natural orbitals were determined by states averaged MCSCF calculations. The sign is of the orbital is indicated by colors (red or blue).

2.1 1st Orbital

LiBe	LiMg	LiCa	LiSr
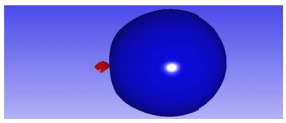	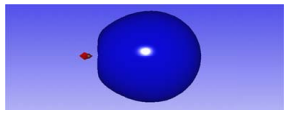	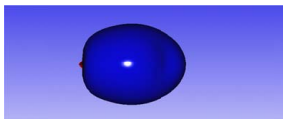	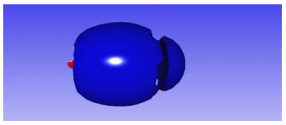
NaBe	NaMg	NaCa	NaSr
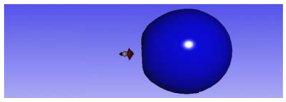	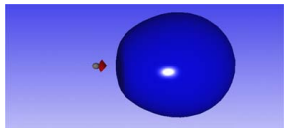	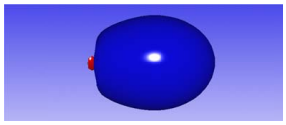	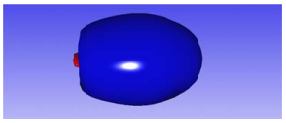
KBe	KMg	KCa	KSr
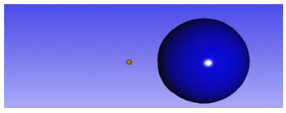	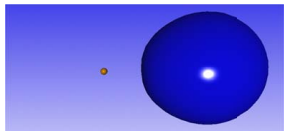	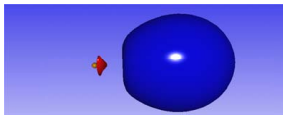	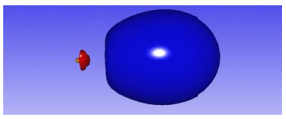
RbBe	RbMg	RbCa	RbSr
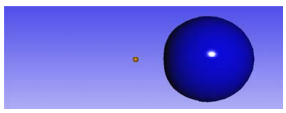	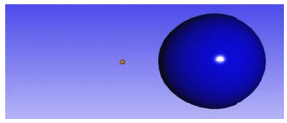	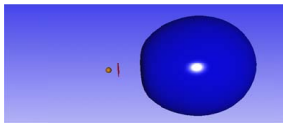	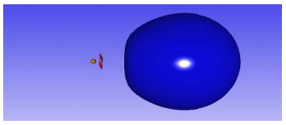

Figure 1: These plots depict the isosurfaces for the first orbital as denoted in Sec. 3.3 and in Fig. 7 in the manuscript. They are isosurfaces of orbitals determined by a state averaged MCSCF calculation. [12]

2.2 2nd Orbital

LiBe	LiMg	LiCa	LiSr
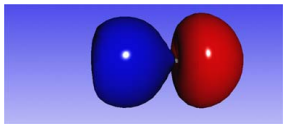	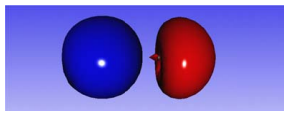	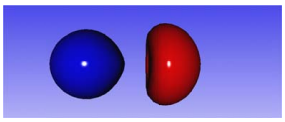	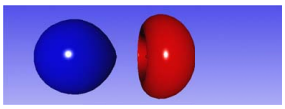
NaBe	NaMg	NaCa	NaSr
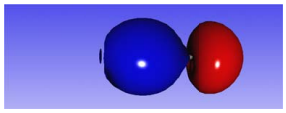	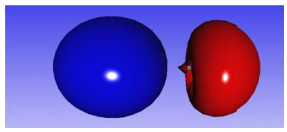	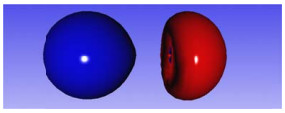	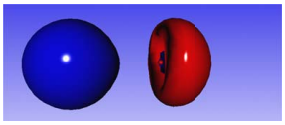
KBe	KMg	KCa	KSr
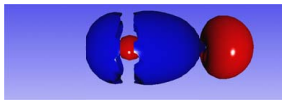	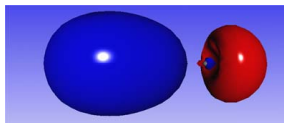	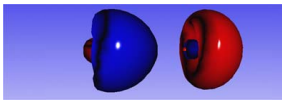	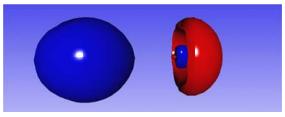
RbBe	RbMg	RbCa	RbSr
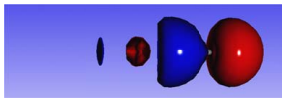	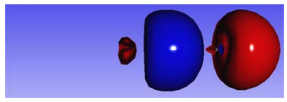	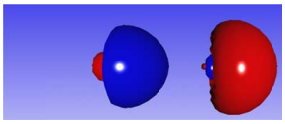	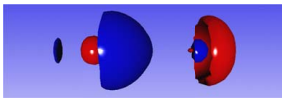

Figure 2: These plots depict the isosurfaces for the second orbital as denoted in Sec. 3.3 and in Fig. 7 in the manuscript. They are isosurfaces of orbitals determined by a state averaged MCSCF calculation.[12]

2.3 3rd Orbital

LiBe	LiMg	LiCa	LiSr
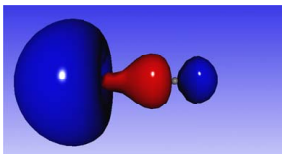	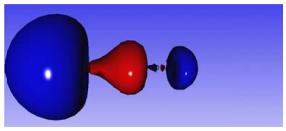	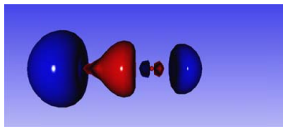	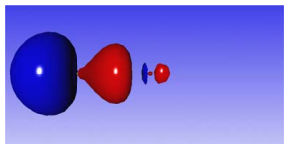
NaBe	NaMg	NaCa	NaSr
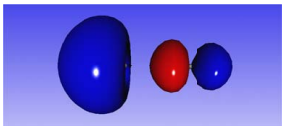	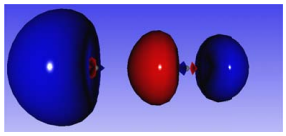	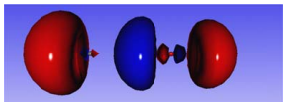	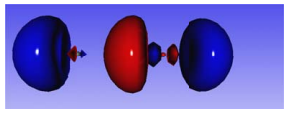
KBe	KMg	KCa	KSr
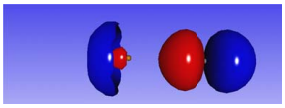	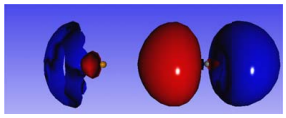	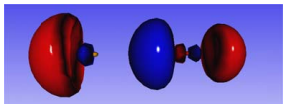	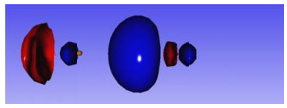
RbBe	RbMg	RbCa	RbSr
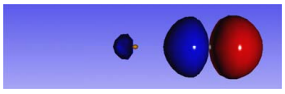	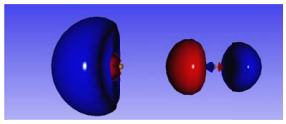	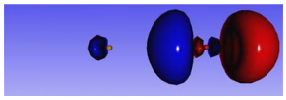	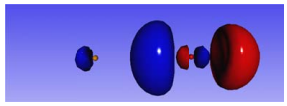

Figure 3: These plots depict the isosurfaces for the third orbital as denoted in Sec. 3.3 and in Fig. 7 in the manuscript. They are isosurfaces of orbitals determined by a state averaged MCSCF calculation.[12]

References

(1) Gopakumar, G.; Abe, M.; Kajita, M.; Hada, M. *Phys. Rev. A* **2011**, *84*, 062514.

(2) Gou, D. Z.; Kuang, X. Y.; Gao, Y. F.; Huo, D. M. *J. Chem. Phys.* **2015**, *142*, 034308.

(3) Allouche, A. R.; Aubert-Frécon, M. *J. Chem. Phys.* **1994**, *100*, 938–944.

(4) Boutassetta, N.; Allouche, A. R.; Aubert-Frécon, M. *Chem. Phys.* **1994**, *189*, 33–39.

(5) Augustovičová, L.; Soldán, P. *J. Chem. Phys.* **2012**, *136*, 084311.

(6) Guerout, R.; Aymar, M.; Dulieu, O. *Phys. Rev. A* **2010**, *82*, 042508.

(7) Cordero, B.; Gomez, V.; Platero-Prats, A. E.; Reves, M.; Echeverria, J.; Cremades, E.; Barragan, F.; Alvarez, S. *Dalton Trans.* **2008**, 2832–2838.

(8) Alvarez, S. *Dalton Trans.* **2013**, *42*, 8617–8636.

(9) Mitroy, J.; Safronova, M. S.; Clark, C. W. *J. Phys. B* **2010**, *43*, 202001.

(10) Ralchenko, Y.; Kramida, A.; Reader, J.; NIST ASD Team, *National Institute of Standards and Technology, Gaithersburg, MD* **2015**, Available: http://physics.nist.gov/asd.

(11) Lide, D. R., Ed. *CRC Handbook of Chemistry and Physics*, 85th ed.; CRC Press, 2004.

(12) Werner, H.-J. et al. MOLPRO, version 2012.1, a package of ab initio programs. 2012; see http://www.molpro.net.